

Kaonic nitrogen X-ray transition yields in a gaseous target

T. Ishiwatari ^a, G. Beer ^b, A.M. Bragadireanu ^{c,e}, M. Cargnelli ^a,
C. Curceanu (Petrascu) ^{c,e}, J.-P. Egger ^g, H. Fuhrmann ^a, C. Guaraldo ^{a,*}, P. Kienle ^a,
T. Koike ^d, M. Iliescu ^{c,e}, K. Itahashi ^d, M. Iwasaki ^d, B. Lauss ^h, V. Lucherini ^c,
L. Ludhova ^f, J. Marton ^a, F. Mulhauser ^f, T. Ponta ^e, L.A. Schaller ^f, R. Seki ^{i,j},
D.L. Sirghi ^{c,e}, F. Sirghi ^c, P. Strasser ^d, J. Zmeskal ^a

^a Institute for Medium Energy Physics, Boltzmannngasse 3, A-1090 Vienna, Austria

^b Department of Physics and Astronomy, University of Victoria, P.O. Box 3055 Victoria, BC V8W 3P6, Canada

^c INFN, Laboratori Nazionali di Frascati, C.P. 13, Via E. Fermi 40, I-00044 Frascati, Italy

^d RIKEN Wako Institute, RIKEN (The Institute of Physical and Chemical Research), Wako-shi, Saitama 351-0198, Japan

^e Institute of Physics and Nuclear Engineering "Horia Hulubei", IFIN-HH, Particle Physics Department,
P.O. Box MG-6, R-76900 Magurele, Bucharest, Romania

^f Physics Department, University of Fribourg, CH-1700 Fribourg, Switzerland

^g Institute de Physique, Université de Neuchâtel, 1 rue A.-L. Breguet, CH-2000 Neuchâtel, Switzerland

^h Department of Physics, 366 LeConte Hall, University of California, Berkeley, CA 94720, USA

ⁱ W.E. Kellogg Radiation Laboratory, California Institute of Technology, Pasadena, CA 91125, USA

^j Department of Physics and Astrophysics, California State University, Northridge, CA 91330, USA

Received 14 January 2004; accepted 21 April 2004

Available online 28 May 2004

Editor: M. Doser

Dedicated to the memory of Lucien Montanet

Abstract

The first measurement of the yields of three kaonic nitrogen X-ray transitions, using the DEAR (DAΦNE Exotic Atom Research) setup at the DAΦNE collider of Frascati, is reported. The yields are $41.5 \pm 8.7(\text{stat.}) \pm 4.1(\text{sys.})\%$ for the $n = 7 \rightarrow 6$ transition, $55.0 \pm 3.9(\text{stat.}) \pm 5.5(\text{sys.})\%$ for the $n = 6 \rightarrow 5$ transition and $57.4 \pm 15.2(\text{stat.}) \pm 5.7(\text{sys.})\%$ for the $n = 5 \rightarrow 4$ transition at a density $\rho = 3.4\rho_{\text{NTP}}$. By using the experimental yields in an atomic cascade calculation, a 1 to 3% K-shell electron population in the $n = 6$ level was deduced.

PACS: 36.10.Gv; 14.40.Aq; 11.10.Qr

Keywords: Kaonic nitrogen yields; K-shell electron population; Charged kaon mass

* Corresponding author. Tel.: +39-0694032318, fax: +39-0694032559.

E-mail address: carlo.guaraldo@lnf.infn.it (C. Guaraldo).

0370-2693

doi:10.1016/j.physletb.2004.04.055

The study of exotic atoms, formed by capturing low-energy kaons from decay of φ -mesons produced in the e^+e^- collider DAΦNE of Frascati National Laboratories, is being performed by DEAR (DAΦNE Exotic Atom Research) [1]. The main goal of the DEAR experiment is the precise determination of the isospin-dependent $\bar{K}N$ scattering lengths through the measurement of strong interaction shift and broadening of the K_α lines of kaonic hydrogen and deuterium, the latter not yet measured.

In this Letter, the observation of kaonic nitrogen X rays measured during the first stage of the DEAR scientific program is reported. Pressurized cooled nitrogen gas was chosen, because the yield of kaonic nitrogen transitions is high enough to permit a sufficiently fast feedback. The measurement had multiple tasks and deliverables: a feasibility study of the DEAR technique to produce and detect kaonic atoms at DAΦNE; the study of the machine background and the setup performance by optimizing the signal to background ratio; the first measurement of kaonic nitrogen transitions yields.

Although X-ray transitions have been measured in many kaonic atoms [2], no results have been published for nitrogen, apart the recent DEAR ones [3]. See, however, [4]. In the present measurement, a pattern of three lines of kaonic nitrogen was clearly identified. The X-ray yields of the transitions were also determined. By using the experimental yields as input, information on atomic cascade could be obtained. In particular, the residual K-shell electrons population was determined.

Understanding the atomic cascade processes in kaonic nitrogen is especially important due to the possible role of this exotic atom for a precise determination of the charged kaon mass—still an open problem [3]. In fact, the determination of meson masses from the X-ray energies of mesonic atoms requires the measurement of transitions which must not be affected by the strong interaction. The levels involved are therefore of relatively high principal quantum number and are influenced by interaction with the electron clouds. Evaluation of the electron screening requires the knowledge of the status of the electron shells, which is difficult to assess, since it depends on the balance between Auger emission and electron refilling. For solids, the evaluation of electron screening is not straightforward, whereas in gaseous targets a high

degree of ionization was observed in antiprotonic [5] and muonic [6] noble gases (neon, argon and krypton atoms).

Fig. 1 shows a schematic of the DEAR experimental setup. It consists of a beam pipe made from 250 μm aluminum with a 650 μm carbon fiber reinforcement, surrounding the interaction point; a target cell made of low- Z material; charge-coupled devices (CCDs) as X-ray detectors; a vacuum chamber to insulate the cold gas target and the cooled CCDs. Two thin scintillators were mounted on both sides of the beam pipe at the interaction point to detect K^+K^- pairs in coincidence (the kaon monitor [7]), which yields a measurement of the absolute luminosity delivered in the interaction point.

The use of a cryogenic pressurized nitrogen gas at 1.5 bar and 120 K—corresponding to a density $\rho = 3.4\rho_{\text{NTP}}$ —increased the number of kaons stopped in the target and optimized the yields. To reduce fluorescence lines from excitation of materials in the target cell and vacuum chamber they were made of selected low- Z materials. An aluminum alloy (AlMgSi_{0.5}) with the lowest possible manganese content, was chosen for the vacuum chamber. The cylindrical target cell, 12.5 cm in diameter and 14 cm high, was constructed of 75 μm Kapton foils reinforced by thin epoxy-fiberglass bars. Laboratory irradiations of all the setup materials using strong X-ray sources showed the presence of Ca and Sr in the epoxy-fiberglass bars. Au (L-complex) electronic transition showed up as well from the ceramic support of the CCDs. The aluminum bottom had a 100 mm diameter hole through which kaons entered the target gas by passing through a 125 μm Kapton window. Thin Zr and Ti foils, placed on the center of the top plate, emitted in-beam calibration lines.

Due to the finite small crossing angle between electron and positron beams, φ -particles are slightly boosted towards the outside of the DAΦNE rings. Therefore, the momentum of K^+K^- pairs has a small angular dependence. Careful Monte Carlo simulations to optimize kaons stopping and X rays entering the CCDs were performed. The boost effect was compensated by degraders composed of step-like multi-layer Hostaphan foils.

Shielding of the machine background was a major concern to the experiment [8]. As shown in Fig. 1, the interaction region was protected by two lead walls,

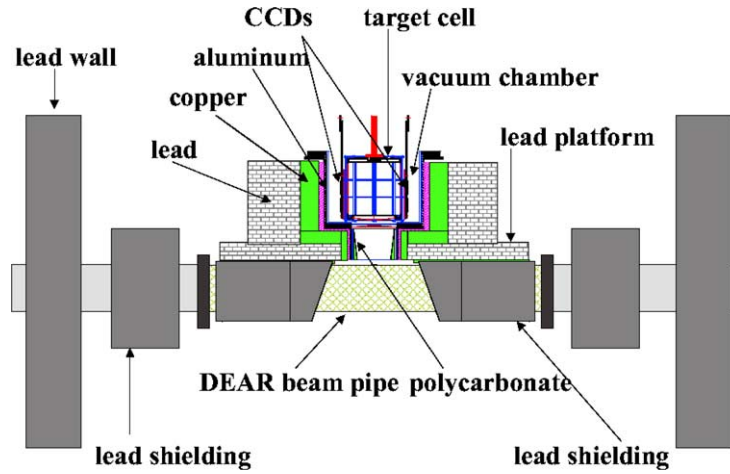


Fig. 1. Schematic figure of the DEAR setup. It consists of a beam pipe surrounding the interaction point at which ϕ s are produced almost at rest, a target cell made of low-Z materials, charge-coupled devices (CCDs) as X-ray detectors, a vacuum chamber to insulate the cold gas target and the cooled CCDs. To reduce low-energy X-ray background a specific shielding technique was adopted.

each 20 radiation lengths thick and 1 m high. Additional lead shielding surrounded the DEAR beam pipe. Using multi-layer packages of materials having decreasing density and atomic number, the low-energy X-ray background generated in the electromagnetic cascades of high energy electrons/positrons from beam loss was reduced by a factor of about 100 in the CCDs.

For X-ray detection, Marconi Applied Technologies CCD55-30 chips were selected. Each CCD55-30 chip has 1152×1242 pixels of $22.5 \times 22.5 \mu\text{m}$, resulting in a total effective area of 7.24 cm^2 per chip. The depletion depth is about $30 \mu\text{m}$. The study of transport and charge integration procedures has shown that the best results in terms of resolution and linearity can be obtained with a readout time of about 90 s. The evaluation of occupancy effect indicates that a total exposure (readout plus static) of 120 s does not significantly reduce the efficiency. Since the amount of data to be collected for each readout was relatively high, a period of 2 minutes was chosen. During the readout the CCDs are exposed and, since no imaging was necessary, the whole acquisition can be done in continuous readout (no static exposure). The target cell was surrounded by 16 CCDs. The CCD-front end electronics and controls, and the data acquisition system, were specially made for this experiment [9].

Data using the nitrogen target were taken for about one month (October 2002), leading to the

optimisation of the setup performance in terms of signal/background ratio. The total collected integrated luminosity was 17.4 pb^{-1} , from which 10.8 pb^{-1} taken with stable conditions were selected for the analysis of the energy spectrum. No cuts were applied to the recorded CCD raw-data.

The CCD detector provides an opportunity to set a characteristic X-ray flag. Since a soft ($\leq 20 \text{ keV}$) X-ray mainly interacts via photoelectric effect, it deposits its energy in the depletion layer into very few pixels. Charged particles or high-energy gamma rays deposit their energy in several adjacent pixels because energy is lost throughout the silicon in the field-free region, where charges can diffuse freely.

The number of hit pixels in a cluster categorizes the event type. In the present analysis, events having 1 or 2 hit pixels were selected as X-ray events, to increase both X-ray detection efficiency and the signal-to-noise ratio. The typical fraction of hit pixels per frame was about 3–5%, such as to have an efficiency of hit recognition of about 98–99%. The X-ray detection efficiency as a function of energy and the X-ray event loss due to pile-up effect were calculated by means of Monte Carlo simulations and laboratory tests. The effect of applying charge-transfer efficiency corrections was an improvement of the resolution from 214 eV FWHM to 176 eV at the K_{α} line of Cu (8040 eV).

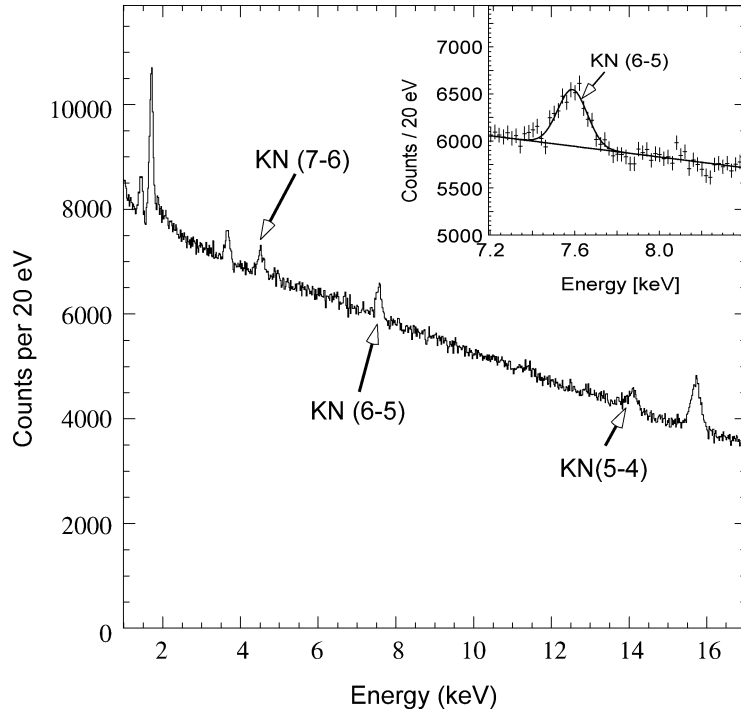


Fig. 2. Energy spectrum of kaonic nitrogen. The arrows show the positions of the kaonic nitrogen X-ray lines: the $7 \rightarrow 6$ transition at 4.6 keV, the $6 \rightarrow 5$ transition at 7.6 keV, and the $5 \rightarrow 4$ transition at 14.0 keV. The peaks at 1.4, 1.7, 3.6, 4.5, 4.9, 11.5, 14.2, and 15.7 keV are the Al-K_α , Si-K_α , Ca-K_α , Ti-K_α , Ti-K_β , Au (L-complex), Sr-K_α , and Zr-K_α lines, respectively. In the insert the fit of the $6 \rightarrow 5$ (at 7.6 keV) kaonic nitrogen transition is reported.

In Fig. 2, the X-ray energy spectrum is shown. Three kaonic nitrogen X-ray lines are well identified. The $n = 6 \rightarrow 5$ kaonic nitrogen transition peak at 7.6 keV is clearly seen. The transition lines $n = 7 \rightarrow 6$ (at 4.6 keV) and $n = 5 \rightarrow 4$ (at 14.0 keV) are overlapped with the Ti-K_α and Sr-K_α lines, respectively. There are no fluorescence X-ray lines around 7.6 keV, thus the kaonic nitrogen peak at 7.6 keV could be fitted with a single Gaussian, as shown in the insert of Fig 2. The FWHM of the $6 \rightarrow 5$ transition line at 7588 eV turned out 161 eV.

The behaviour of the continuous background in Fig. 2 deserves a specific comment. The measured ratio between background levels at 4.6 and 7.6 keV (1.15) is different from the ratio between the X-ray absorption at the two energies in a layer of 30 μm of silicon (2.2). This is mainly due to the structure in space and energy of the incident background, represented by the products of the e.m. cascades in the setup materials. The presence of double pixel hits in the spectra implies also the inclusion of a fraction of events coming

from minimum ionizing particles (MIPs). MIPs produce essentially multiple-pixel events which can be clearly identified in the 4-pixel spectra as a wide bump centered on the corresponding energy deposition of a MIP in a 30 μm silicon layer (about 10 keV). A smaller contribution of MIPs is as well present in the 3- and 2-pixel spectra, as shown in Fig. 4.10.d of Ref. [10]. The net result from the composition of the exponential drop of background due to the decreased absorption with energy and the slight increase for the above effects is a nearly linear decrease over almost the full energy range shown in Fig. 2.

The other two kaonic nitrogen peaks were fitted with multi-Gaussian functions, with energies fixed to known values both for the kaonic transitions and the Ti and Sr fluorescence excitations, to obtain their intensities, as shown in Fig. 3.

To estimate the transition yields, Monte Carlo calculations of kaon stopping efficiency in the target gas, X-ray absorption in gas and in the target windows, and the CCD quantum efficiency were performed.

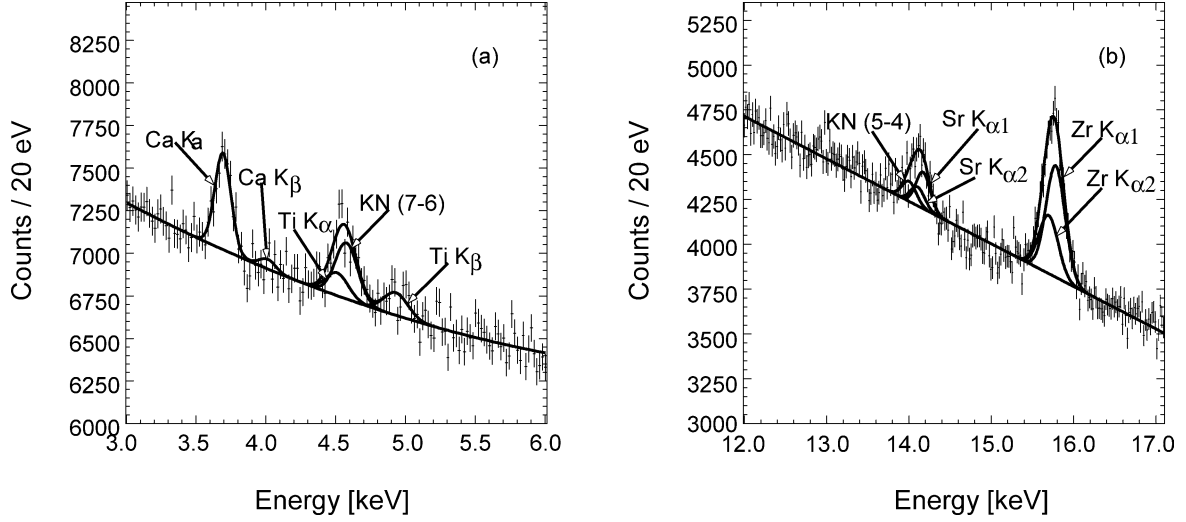


Fig. 3. Fit of the $n = 7 \rightarrow 6$ (at 4.6 keV) and $n = 5 \rightarrow 4$ (at 14.0 keV) kaonic nitrogen transitions. The kaonic peaks and the fluorescence lines are clearly separated.

Table 1

Yields of kaonic nitrogen X rays at a density $\rho = 3.4\rho_{\text{NTP}}$. Measured and Monte Carlo estimated numbers of events assuming a 100% yield are tabulated. The yields are calculated using the experimental values divided by the simulated ones

Transition	$7 \rightarrow 6$	$6 \rightarrow 5$	$5 \rightarrow 4$
Calculated energy (keV)	4.5773	7.5957	13.9996
Measured number of events	3310 ± 690	5280 ± 380	1210 ± 320
Predicted number of events	7971 ± 796	9590 ± 962	2108 ± 210
Yield	$41.5 \pm 8.7(\text{stat.}) \pm 4.1(\text{sys.})\%$	$55.0 \pm 3.9(\text{stat.}) \pm 5.5(\text{sys.})\%$	$57.4 \pm 15.2(\text{stat.}) \pm 5.7(\text{sys.})\%$

Table 1 contains a summary of the results for the yields of the $7 \rightarrow 6$, $6 \rightarrow 5$ and $5 \rightarrow 4$ kaonic X-ray transitions in nitrogen. The measured number of events in the corresponding lines is compared with the predicted number of events from Monte Carlo simulations in which the yields were assumed to be 100%. The systematic error of the calculation was estimated to be about 10%. In the last line of Table 1 the final results of the observed yields including statistical and systematic errors at a density $\rho = 3.4\rho_{\text{NTP}}$ are reported. There is a tendency that the yield increases in going from the $7 \rightarrow 6$ to the $6 \rightarrow 5$ and $5 \rightarrow 4$ transitions.

Using our measured values for the transition yields as input, a cascade calculation was performed to evaluate the screening effect due to the K- and L-shell electron population. In exotic atoms with $Z > 2$, the deexcitation takes place in a competition mainly between the internal Auger effect and radiative transi-

tions, and the electron population is determined as the consequence of a balance between Auger emission and electron refilling. The Auger transition rates for emitting K- and L-shell electron for the case of filled shells were evaluated by first order perturbation theory [11,12]. During the cascade, the actual Auger rate varies with the number of electrons. In the present cascade model, both K- and L-shell electron refilling processes were taken into account. In a gas target at the present density, the L-shell refilling is expected to be negligibly small compared to other processes because of the low collision rate with surroundings.

The cascade calculation starts from $n \sim 30$ with a modified statistical distribution $P(l) \propto (2l + 1) \times \exp(-al)$, where a is a free parameter. The electron refilling rates for K- and L-shells are also free parameters in the present calculation, as well as the shell filling probabilities at start.

Table 2

Best-fitted cascade parameters in the χ^2 -fit to the X-ray yields and their uncertainty within 1σ

K-shell refilling rate	$(1.10^{+1.22}_{-0.03}) \times 10^{12} \text{ s}^{-1}$
L-shell refilling rate	$(0.00^{+0.01}_{-0.00}) \times 10^{12} \text{ s}^{-1}$
Initial K-shell filling probability	$0.15^{+0.15}_{-0.01}$
Initial L-shell filling probability	$0.49^{+0.11}_{-0.08}$
a [in $\exp(al)$]	0.05 ± 0.01

Table 3

Calculated X-ray yields for $\Delta n = 1$ and $\Delta n = 2$ transitions using the best-fitted cascade parameters given in Table 2

$7 \rightarrow 6$	41.2%	$8 \rightarrow 6$	6.4%
$6 \rightarrow 5$	49.0%	$7 \rightarrow 5$	7.2%
$5 \rightarrow 4$	56.8%	$6 \rightarrow 4$	6.9%
$4 \rightarrow 3$	64.0%	$5 \rightarrow 3$	6.0%

The nuclear absorption rate was obtained by numerically solving the Klein–Gordon equation with the phenomenological K^- -nucleus potential of Ref. [13]. In this potential, several nuclear bound states appear below the atomic states, but the transition to such nuclear state is ignored. In the circular orbit, nuclear absorption dominates for $n \leq 3$ states.

The cascade parameters were adjusted to reproduce the experimental yields. The best-fitted cascade parameters with their uncertainties are reported in Table 2. Since the $8 \rightarrow 6$ X-ray energy transition (about 7.55 keV) is very close to the $6 \rightarrow 5$ one, the fit was done by assuming that the observed “ $6 \rightarrow 5$ ” yield is the sum of the $6 \rightarrow 5$ and $8 \rightarrow 6$ yields. The calculated X-ray yields using the best fit cascade parameters are shown in Table 3.

As for the L-shell refilling rate is concerned, an eventual conflict between thermalization and Coulomb explosion, as observed in the case of pionic nitrogen [14], does not show up at the presently achieved accuracy and within the present cascade model. It should be examined by using more elaborate cascade models, using a L-shell refilling rate depending on the velocity and the charge of the kaonic atoms.

Within the uncertainty of the parameters in Table 2, it is found that for the $n = 6$ level a K-shell electron fraction of approximately 1–3% is expected in the present cascade approach. After the kaon cascades along the circular orbits, the kaonic atom is almost

completely ionized at $n = 6$ and no refilling occurs at $n \leq 6$. The transitions from the $\Delta n = 2$ non-circular orbits, where the K-shell refilling is important, contribute to the K-shell electron fraction, but it seems doubtful to conjecture their contribution in view of the simple model used. The residual population is important to be measured because cascade calculations still need a lot of experimental inputs to fine tune all the involved rates to fit observables.

Jensen independently performed a cascade calculation for kaonic nitrogen and the K-shell electron population was estimated to be $\sim 2\%$ at $n = 6$ [15], in agreement with our cascade results.

The measured energy of the $n = 6 \rightarrow 5$ transition was precisely determined to be 7.588 ± 0.005 (stat.) keV. Ti and Zr foils were placed inside the setup with the specific goal of energy scale calibration, but in reality all electronic transitions were used to calibrate the energy scale and to check the linearity. Especially the Ca transitions (free from interference with kaonic nitrogen transitions) were particularly useful for this aim. No systematic effect is coming from the process of energy calibration.

The $6 \rightarrow 5$ energy transition value could be used to evaluate the charged kaon mass from the first order of the Klein–Gordon equation using a point-like nucleus, resulting in:

$$M_{K^-} = 493.884 \pm 0.314(\text{stat.}) \text{ MeV.}$$

This results represents an improvement of one order of magnitude in precision with respect to our preliminary result obtained with a prototype setup [3], mainly due to the improvement of the signal to noise ratio. It implies that the precision on the kaon mass determination can be improved if a detector system having better resolution than CCDs, together with a further background reduction, is used [3].

In conclusion, the first measurement of the yields of three kaonic nitrogen X-ray transitions: $n = 7 \rightarrow 6$ at 4.6 keV; $n = 6 \rightarrow 5$ at 7.6 keV; $n = 5 \rightarrow 4$ at 14.0 keV was performed. The yields were determined from the observed events together with the Monte Carlo simulation to estimate efficiencies of kaon stopping and X-ray detection. The determined yields are:

$$41.5 \pm 8.7(\text{stat.}) \pm 4.1(\text{sys.})\%$$

for the $n = 7 \rightarrow 6$ transition,

$55.0 \pm 3.9(\text{stat.}) \pm 5.5(\text{sys.})\%$

for the $n = 6 \rightarrow 5$ transition,

$57.4 \pm 15.2(\text{stat.}) \pm 5.7(\text{sys.})\%$

for the $n = 5 \rightarrow 4$ transition.

Comparison of the experimental yields with an atomic cascade calculation showed a 1–3% residual K-shell electron population at a density $\rho = 3.4\rho_{\text{NTP}}$.

Acknowledgements

We want to remember with affection and gratitude our great friend Lucien Montanet, who has followed since the beginning the exotic atom researches at DAΦNE in Frascati giving us enlightening suggestions. The DEAR Collaboration wishes to thank the DAΦNE machine crew for their friendly cooperation. This research was partially supported by European Community, Access to Research Infrastructure, contract number HPRI-CT 1999-00088, and partially supported by the Swiss National Science Foundation.

One of the authors (T. Koike) is supported by the Special Postdoctoral Researchers Program from RIKEN.

References

- [1] S. Bianco, et al., Riv. Nuovo Cimento 22 (1999) 1.
- [2] C.E. Wiegand, G.L. Godfrey, Phys. Rev. A 9 (1974) 2282; C.J. Batty, Sov. J. Part. Nucl. 13 (1982) 71.
- [3] G. Beer, et al., Phys. Lett. B 535 (2002) 52.
- [4] G. Godfrey, Ph.D. Thesis, Univ. of California, 1975, unpublished.
- [5] R. Bacher, et al., Phys. Rev. A 38 (1998) 4395.
- [6] R. Bacher, et al., Phys. Rev. A 39 (1989) 1610.
- [7] V. Lucherini, et al., Nucl. Instrum. Methods A 496 (2003) 315.
- [8] M. Bragadireanu et al., DEAR Technical Note IR-37 (2001).
- [9] M. Iliescu, et al., Nucl. Instrum. Methods, in preparation.
- [10] T. Ishiwatari, Ph.D. Thesis, RIKEN, 2004.
- [11] G.R. Burbidge, A.H. de Borde, Phys. Rev. 89 (1953) 189.
- [12] A.H. de Borde, Proc. Phys. Soc. A 67 (1954) 57.
- [13] C.J. Batty, E. Friedman, A. Gal, Phys. Rep. 287 (1997) 385.
- [14] T. Siems, et al., Phys. Rev. Lett. 84 (2000) 4573.
- [15] T.S. Jensen, DEAR Technical Note IR-45 (2003); T.S. Jensen, private communication, 2003.